Towards accurate stereo-video based free-surface reconstruction for wave tank experiments

IOP Conf. Series: Materials Science and Engineering 1288 (2023) 012009 doi:10.1088/1757-899X/1288/1/012009

Towards accurate stereo-video based free-surface reconstruction for wave tank experiments

Sacha Le Page[1], Alan Tassin[1], Julien Caverne[1], Yves Le Gall[1], Benoit Gomez[1], Guillaume Ducrozet[2]

[1]Ifremer, RDT Research and Technological Development, F-29280 Plouzané, France
[2]Nantes Université, École Centrale Nantes, CNRS, LHEEA, UMR 6598, F-44000 Nantes, France

E-mail: slepage@ifremer.fr

Abstract. Measuring accurately the shape of the free surface in medium-scale hydrodynamic testing facilities is challenging with conventional wave gauges. To overcome this problem, it is necessary to go towards higher resolution measurement systems. For this purpose, we investigate the ability of stereo-video acquisition systems to reconstruct free surface waves in laboratory conditions. This technique has been proven to give satisfactory results in open sea conditions, although it is dependent on the environmental conditions (weather, solar incidence angle). At sea, the stereo-video reconstruction algorithm makes profit of the short waves generated by the wind in order to correlate the points from the left and right images. The main challenge of adapting this technique to laboratory conditions, *i.e.* in absence of sun and wind, is to overcome the absence of texture on the free surface. This paper presents recent work aiming at developing a stereo-vision measurement system for laboratory conditions. Our efforts have been devoted to finding an adapted lighting system and generating a texture suitable for the reconstruction algorithm. Different lighting configurations have been tested in order to understand its impact on the reconstructions. For the texture generation, we have investigated different means of generating short surface waves (water droplets, air blowing, circulation current, underwater acoustic emissions) in different experimental facilities. Our conclusions show that it is possible to reconstruct the shape of surface gravity waves in the presence of short surface waves and that the effects of lighting and texture on the quality of the reconstruction are strongly coupled.

1. Introduction

Wave-structure interaction is still a challenging field of research with stimulating engineering applications. There has been a lot of efforts dedicated to the development of non-linear wave-wave interaction models and non-linear wave-structure interaction models in the last decades. From an experimental point of view, these phenomena are also challenging to investigate in wave tanks, as they require innovative developments in terms of measurements. Indeed, one may be interested in having a better spatial description of the free-surface profile, tracking the evolution of the wetted surface and measuring high-frequency force components induced by higher-order wave-structure interactions. Regarding the measurement of the free-surface, there has been several attempts to improve the resolution of the measurements. Baldock & Swan [1] proposed a non-linear reconstruction method based on a punctual free-surface elevation measurement and a double Fourier series expansion of the velocity potential and of the free-surface elevation. This method has been revisited recently by Carciunescu & Christou [2], showing interesting results

up to mildly breaking waves. Until recently, the only way of getting a refined measurement of the wave field was to deploy tens of wave gauges and to repeat the experiments with the wave gauge rack at different locations, as performed by Swan & Sheikh [3] who have measured the wave elevation around a vertical cylinder at 1400 locations. In narrow wave flumes, it is possible to visualize the free-surface profile with a video camera by tracking the intersection at the wall [4] or by a side view through a glass wall [5], but the wave profile along the wall is affected by the presence of the wall. For more complex wave fields, it is necessary to use set-ups with two or more video cameras. Aubourg *et al.* [6] used a stereo-PIV set-up with 3 cameras making it possible to measure the wave field and the velocity field at the free surface. A stereo-refraction approach was used by Gomit *et al.* [7] to measure the wave field while a stereo-thermal PIV approach was used by Savelyev & Fuchs [8] to measure the free-surface elevation and the velocity field at the free surface. The stereo-PIV method requires seeding in the fluid with floating particles which may be missing in certain areas (*e.g.* wake of a ship, behind the crest of a breaking wave, or due to a segregation process). Stereo-refraction is very sensitive to small deformations of the free-surface but is not adapted to steep waves. Stereo-thermal PIV requires infra-red cameras and a powerful infra-red laser, which is expensive and presents safety issues for users. In the present paper, we investigate the feasibility of stereo-video reconstruction in a wave tank using short waves at the free-surface. This approach tends to reproduce the principles of stereo-video wave measurement at sea using WASS, an open-source stereo processing pipeline developed by Bergamasco *et al.* [9] and Benetazzo *et al.* [10, 11]. We report here on different experiments which have been carried out for that purpose. The paper is organised as follows: **section 2** presents a first attempt to reconstruct a free-surface with short waves, **section 3** investigates the effect of the lighting set-up on the reconstruction and **section 4** investigates the feasibility of using underwater ultrasonic transducers to generate short free-surface waves. Finally, some conclusions are drawn in **section 5**.

2. Reconstruction of the free-surface from shortwaves: influence of the texture generation

This section aims to show the influence of the texture generation on free-surface reconstruction via observations made during an experimental campaign at the wave and current flume tank of IFREMER located in Boulogne-sur-Mer (Pas-de-Calais, France).

2.1. Experimental Set-up

The working section of the facility is 4m wide, 18m long and 2m deep. The facility is filled with freshwater, it can generate current up to 2m/s and waves can be superimposed to the current. In our case, the wave maker was located upstream, generating waves propagating in the same direction as the current. The tank is equipped with a 4m by 4m false floor that can be lifted up to a few centimeter above the free surface. Images of the experimental setup are shown in **Fig. 1** and a side view sketch is shown in **Fig. 2**.

Two high-speed cameras (PHOTRON Mini AX, 1024x1024 pixel) with 35mm lenses are installed 1.74m above free surface, in the median axis of the flume, with a 33° angle to the horizontal. The baseline, *i.e.*, the distance between both cameras optic center, is about 577 mm.

A large translucent screen (a polyane tarpaulin) is hung over an overhead crane positioned 7m ahead of the cameras, both layers are spaced from 20cm. With a 3.6m height and a 6m width, the tarpaulin provides a large screen to uniformly illuminate the free surface. To prevent direct lighting on the screen, (unfavorable to stereo-video reconstruction) the latter is lit by retro-lighting, *i.e.*, two LED lighting heads are placed behind the screen and oriented towards the white ceiling.

The stereo camera calibration is done with a 405x360mm chessboard using MATLAB Stereo Camera Calibrator [12], inspired by Bouguet [13], Zhang [14], and Heikkila et al [15]. The

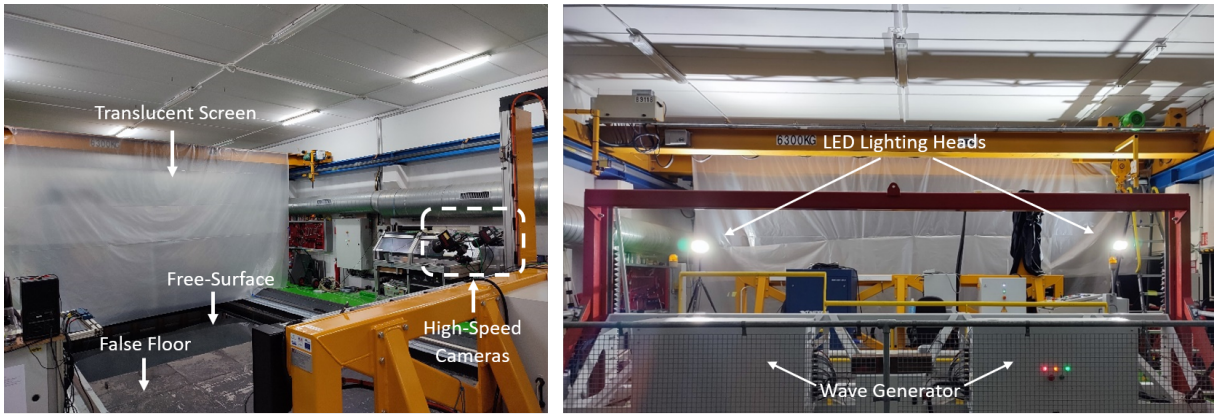

Figure 1. Boulogne-sur-Mer experimental campaign setup. On the left: Experimental setup on the cameras side. On the right: Setup, behind the translucent screen

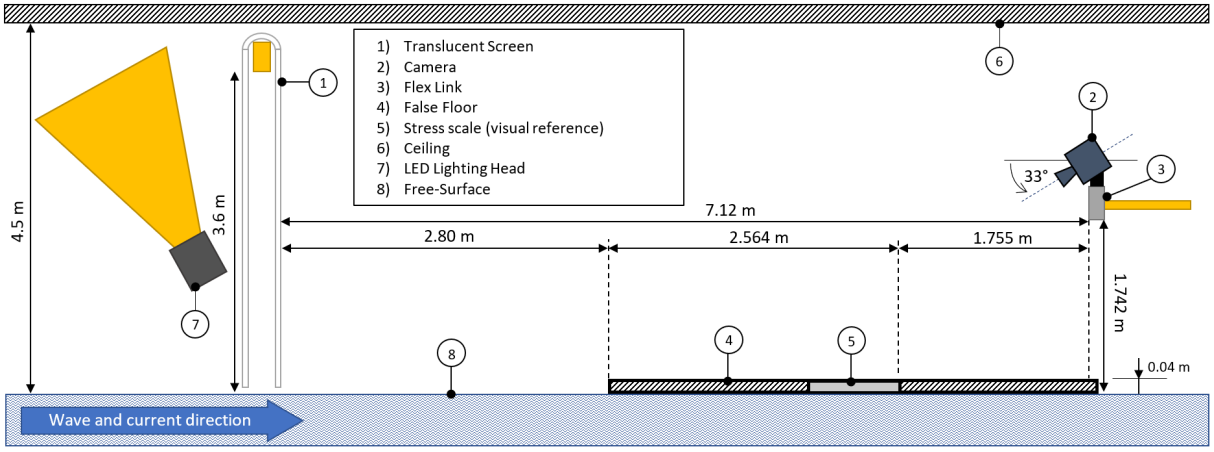

Figure 2. Boulogne-sur-Mer experimental campaign setup. Side view scheme

results show that both cameras have low distortion and the reprojection error is very low (about 0.04 px). In order to assess the accuracy of the stereo-video reconstruction, the false floor is reconstructed using the WASS pipeline. As the false floor is allegedly planar, a comparison of the altitudes of the reconstructed points with a median plane gives an estimate of the accuracy of the setup. **Fig. 3** shows the rectified pair of images used for the reconstruction of the false bottom. Some epipolar lines are displayed in red over the pair of images. **Fig. 4** shows the 3D reconstruction of the false floor. Each calculated point is given the "color" (in gray scale) of the associated pixel on the pair of pictures, which gives a rather realistic render to the reconstruction. Removing outliers, the point cloud can easily be compared to a median plane. The analysis of the altitude of the points around this plane gives an error of standard deviation from the median plane of $2.7mm$.

In order to generate texture, we take advantage of the short waves induced by the water circulation in the flume. After testing several current velocities (from 0.5 m/s to 1 m/s), it appears that a water circulation of 0.7 m/s gives the best results in terms of calm (no waves) free-surface reconstruction without altering the free-surface shape too much. Unfortunately, when regular waves are generated in the flume, huge gaps remain in the middle of the reconstructed

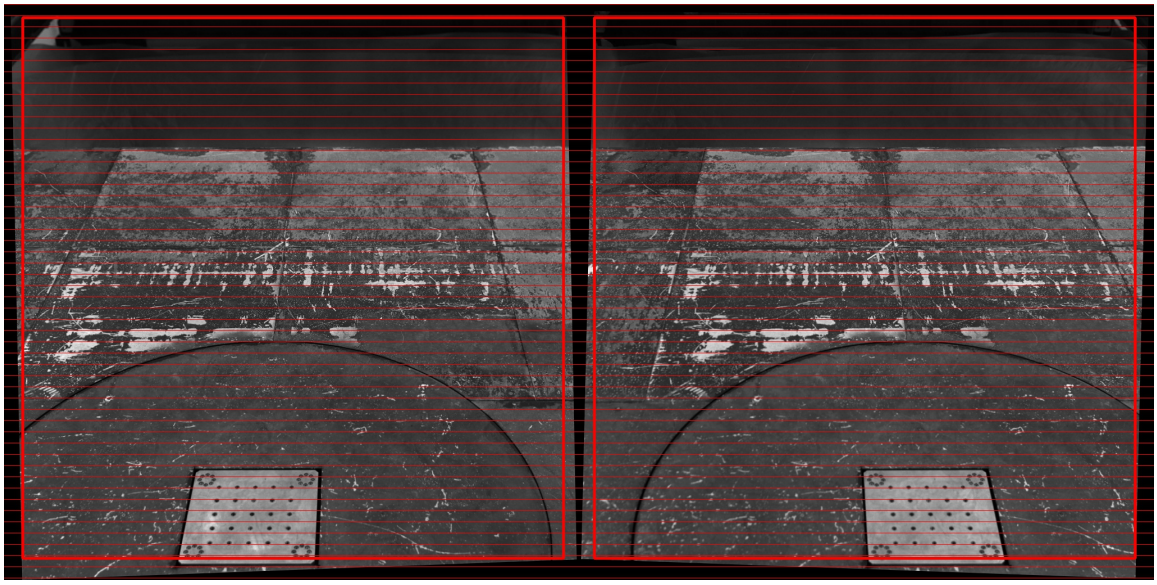

Figure 3. Rectified pair of images of the false floor, used for 3D reconstruction

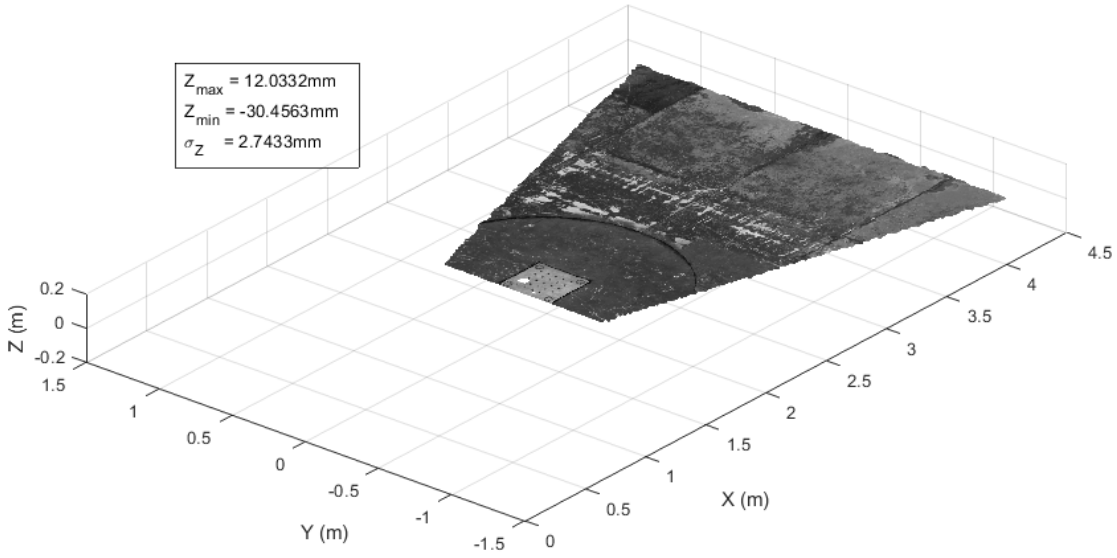

Figure 4. 3D reconstruction of the false floor (point cloud). The points beyond X=4.3m are considered as outliers and have been removed (X=0 is the position of the cameras)

zone indicating that the texture generated by the water circulation is not enough for accurate free-surface reconstruction with waves.

With a view to extend the surface of reconstruction and to improve the accuracy of the reconstruction, three additional means of generating texture at the free-surface are investigated. Firstly, a rope is tied above the flume, flicking the free-surface, so the impact between the rope and the circulating water generates short waves. Secondly, water droplets are projected over the surface by means of a hose pipe. Finally, through the use of a blow gun, compressed air is projected on the free-surface.

The addition of compressed air projection to water circulation gives the best results in terms of reconstructed surface extension and accuracy increase. **Fig.5** shows the reconstruction of regular waves (crest-to-trough wave height H=0.22m, wave period T=1.33s) at four different instants over a period. For this reconstruction, the video is acquired with a 10 Hz frame rate. Reconstructions produced with those conditions allow to observe an entire wavelength ($\lambda = 2.76m$) at different time. The free-surface reconstructions are shown as point clouds directly generated by WASS (same as **Fig. 4**). One observes that almost all the field covered by the stereo-rig is fully reconstructed, except the furthest points to the cameras (about 4.6m from the cameras) that are not well reconstructed. This is due to the fact that the translucent screen does not fall up to the free surface, hence there is a band on the free surface that is not illuminated from the point of view of the cameras. The results is quite satisfactory as it confirms that free surface reconstruction with waves is possible with fine texture generated by short waves. Moreover, the reconstruction seems accurate as the measured crests to troughs distance is of the same magnitude as the set value.

2.2. Tests with compressed air blowing only

Following the positive results obtained with the texture generated by current and compressed air blowing, another test is done on a calm free surface, *i.e.*, without water circulation nor waves. **Fig.6** shows on the right image a left camera view of the free surface, so one can observe the short waves generated by the compressed air blowing. On the left image, the green area refers to the reconstructed points. The right part of the surface is not reconstructed, nor is the top part, due to the lack of texture. The left part is not reconstructed because it is out of the right camera field. The bottom part lacks lighting (the screen does not go high enough) so texture is harder to distinguish letting the floor of the tank visible. As it is difficult to uniformly generate short waves on the measured free-surface using a single blow-gun from the edge of the flume, other reconstructions are done after changing the location of the impact of the air projection. For example, we managed to reconstruct the non-reconstructed area on the right in **Fig.6** by moving the air impact closer to this zone, to the detriment of the reconstruction of the left side. That is to say that with a correct lighting one can sensibly advocate that the more dense and shorter the short waves are, in a specific area, the better the reconstruction will be in this area. Adding texture on free-surface allows to "hide" the bottom of the tank that is seen through the water due to the angle of incidence of the cameras (especially close to the cameras).

After a few outliers removal on the reconstruction obtained with pictures from **Fig.6**, the standard deviation of the altitude (z-coordinate) around a horizontal median plane drops to $\sigma_Z = 7.38mm$. This error on the altitude is quite encouraging and shows the free-surface reconstruction is rather flat, given that the short waves generated by the pressurized air blown are a few millimeters high.

2.3. Regular waves reconstruction (texture generated by compressed air projection)

To conclude the experimental campaign performed in the Boulogne-sur-Mer facility to investigate the feasibility of free-surface reconstruction using short waves as texture, the reconstruction of three different regular waves condition has been tested: H=0.048m, T=0.67s ; H=0.05m, T=0.56s and H=0.048m, T=0.5s. The texture is once again generated by compressed air projection on the free surface. The air flow is located 2m away from the camera as it seems to be the best compromise to have both a large surface reconstruction and a dense point cloud. All three reconstructions cover almost all of the filmed free surface, *i.e.*, a 3m high trapezoid with bases going from 1.5m to 3m.

It is noticed that the shorter the period is, the less troughs are seen by the cameras hence reconstructed. As the period decreases, the wave curvature increases and favours the troughs masking by the crests. On **Fig. 7**, showing the reconstruction of (H=0.05m, T=0.56s), the first

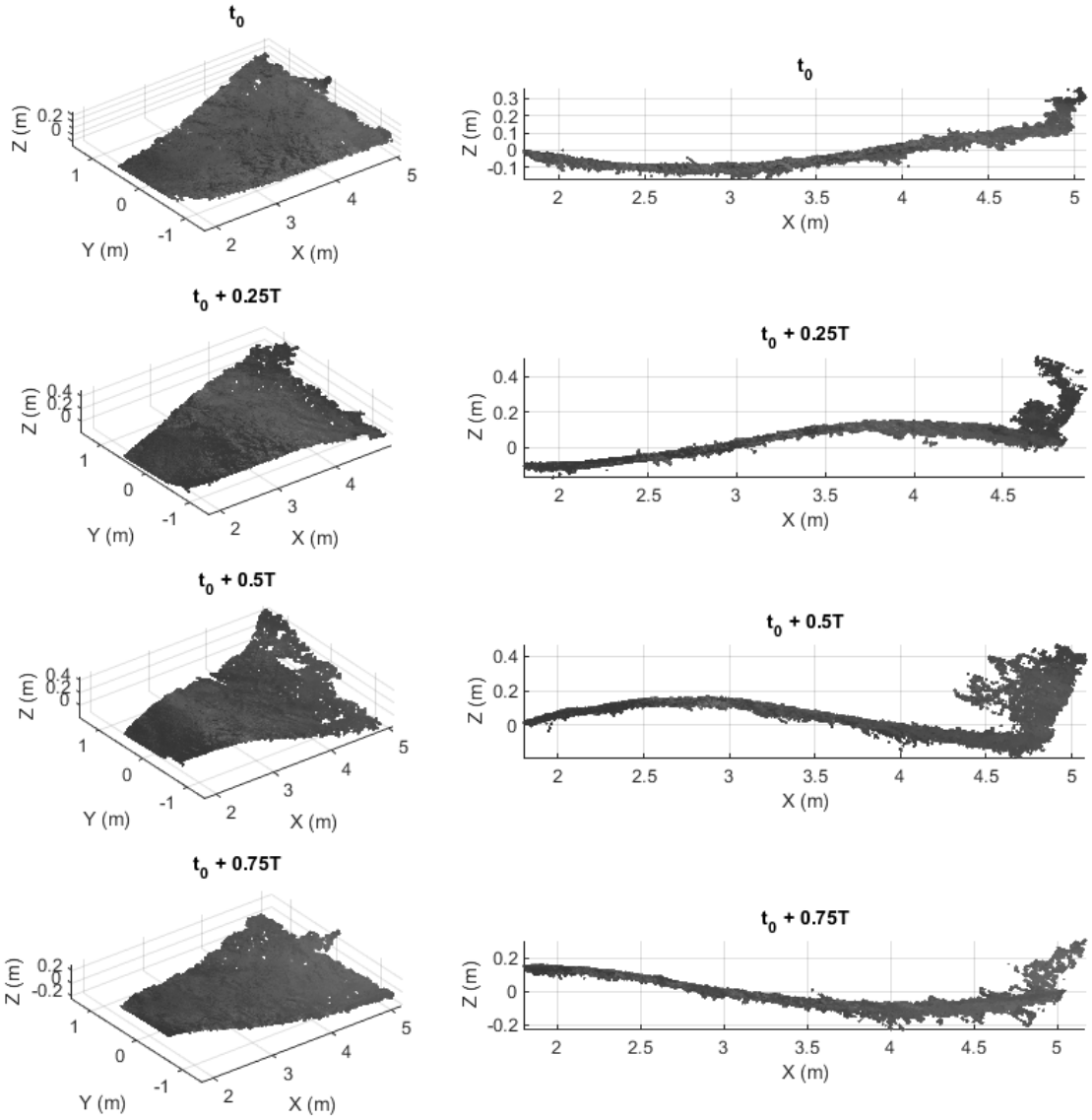

Figure 5. 3D reconstructions (point cloud) of regular waves (H=0.22m, T=1.33s) with current ($V_c = 0.7m/s$) and compressed air projection

two wave lengths, extending along 1.5m, are entirely reconstructed. Then, the crest masking effect takes precedence and troughs are no longer reconstructed. On the side view (**Fig. 7** right image), it seems that all the observed crests and troughs are fully reconstructed, but a change of viewing angle (left image) shows gaps between the further crests.

Nonetheless, the results of those tests are promising and show that with appropriate lighting and fine texture, free-surface reconstruction and waves measurement in test tanks are possible on an approximately 3m by 3m surface. However, the tests also showed some limitations in our process, namely the troughs masking, but they might be avoided by setting the cameras perpendicularly to the waves principal direction.

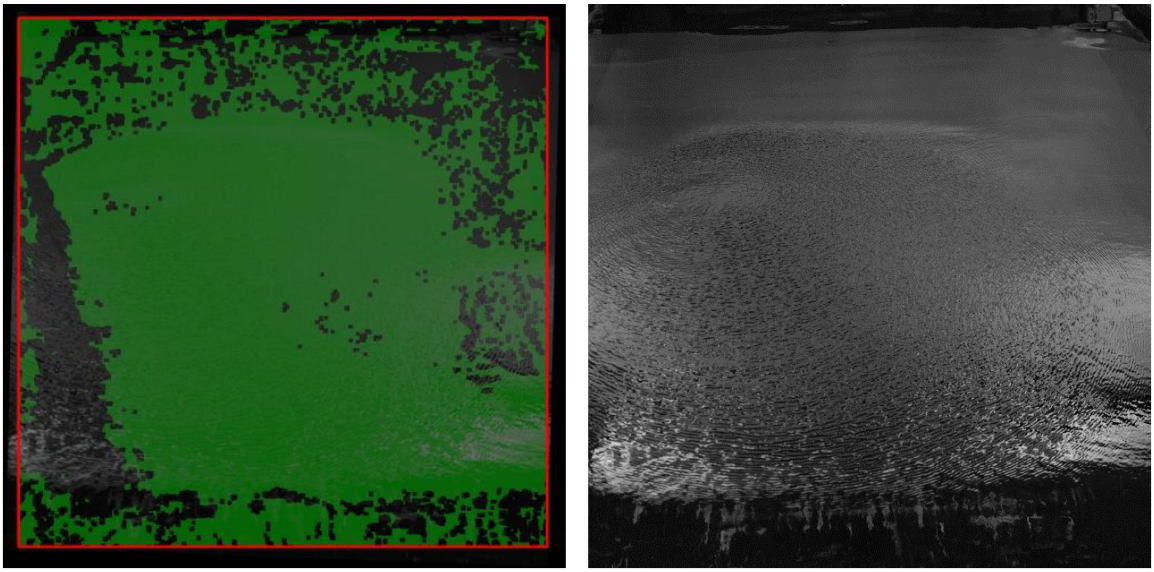

Figure 6. On the right: Calm free surface textured by compressed air blowing (left camera view), on the left: reconstructed zone

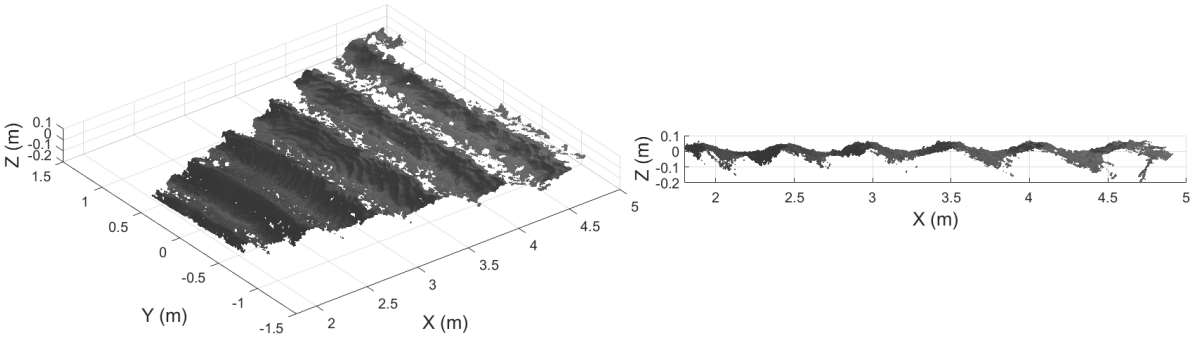

Figure 7. Regular waves reconstruction (H=0.05m, T=0.56s)

3. Reconstruction of the free-surface from shortwaves: influence of the lighting setup

Following an experimental campaign principally focused on texture generation and its influence on stereo video based free-surface reconstruction, a second experimental campaign was conducted at the wave flume of IFREMER located in Plouzané (Brittany, France), to have a better understanding of the influence of the lighting set-up. The main idea for this campaign is to create, over the flume, an artificial sky (AS) that would deliver a uniform and diffuse lighting on the observed free-surface.

3.1. Experimental Set-up

The flume is 50m long, 4m large and 3 meter deep. The side walls go about 1 m high above the free-surface. For this campaign, the same cameras and lenses were used and placed in a similar way as previously. The cameras are installed in the median axis of the flume, 1.9m above the still free-surface, on a footbridge. They are oriented towards the free surface with a 38° angle to

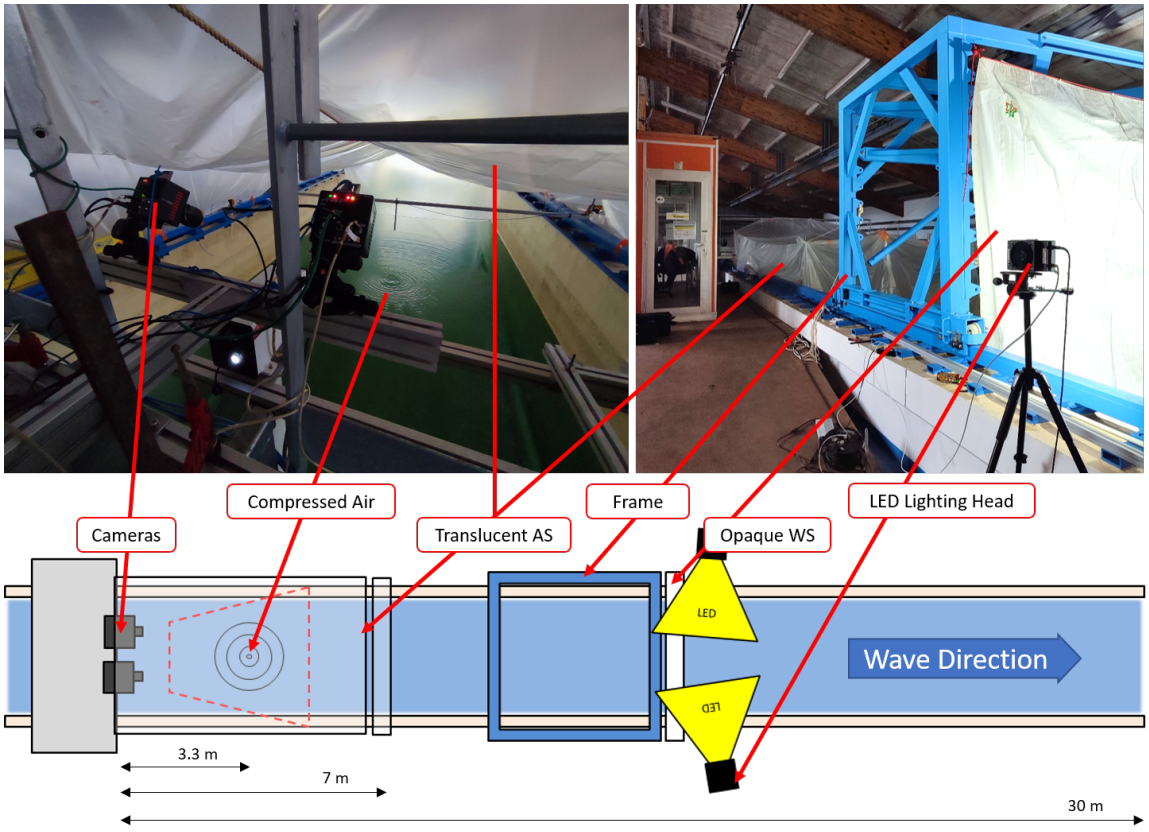

Figure 8. Experimental set-up with translucent artificial sky (AS) and opaque white screen (WS) (Config. 2)

the horizontal and the baseline is again 577 mm. The stereo camera calibration is done with the same technique and gives once again a very low reprojection error (0.04 px). As compressed air projection on the surface has been proven to be our best way to generate short waves, hence fine texture on the free surface, a small flexible pipe ($\varnothing 6mm$) supplied with compressed air is placed above the flume, 3.3m away from the cameras. The pressure of the compressed air distribution network is lower than at the facilty in Boulogne-sur-Mer hence the pipe was installed vertically, about 1m above the free-surface. It creates a source point, right under the pipe, from which short waves propagates. This installation compromises between having a decent texture and keeping the pipe out of the cameras' field, nonetheless, the generated texture is less fine than the one obtained in Boulogne-sur-Mer. **Fig.8** shows two pictures and a top view scheme of the set-up.

The previously mentionned artificial sky is set-up either by hanging the same translucent polyane tarpaulin used in Boulogne-sur-Mer (**Config. 1 and 2**, see **Tab.1**), or more opaque white screens coming from boat sails (**Config. 3**) over the flume. The artificial sky is hung by means of ropes, tensed from the previously mentioned footbridge to a large frame that can be moved along the flume. It goes over the cameras and extends to 7m in front of them. Both sides are also covered as the artificial sky drops to the flume walls. The artificial sky hence forms a tunnel, however, due to its own weight and accessibility issues it cannot be properly taut and many folds appear, as it can be seen on **Fig.8**. The end of the tunnel is "closed" on the opposite side of the cameras to prevent direct lighting on the surface, highly unfavorable to stereo-video reconstructions.

In total, reconstructions with 88 different configurations have been tested by modifying the artificial sky set-up and by playing with the lighting conditions (adding a diffusive screen, changing the location and orientation of the lighting heads). Those configurations can be summarised in three main set-up configurations. In the first configuration, the artificial sky is entirely composed with translucent tarpaulins. The addition of a large opaque white screen (WS) to diffuse the light, hung across the width of the flume in front of the artificial sky, forms the second configuration. It is the configuration represented on the pictures and scheme in **Fig.8**. The third and last configuration consists in an artificial sky only made with opaque white screens only (same material as the diffusing screen). **Tab. 1** sums up the main set-up configurations to which this paper will refer to.

Table 1. Main set-up configurations for lighting influence studies

	Artificial Sky (AS)	Light Diffusion Screen
`Config.1`	Translucent	No
`Config.2`	Translucent	Yes: Opaque White Screen
`Config.3`	Opaque	No

3.2. Influence of the artificial sky on the reconstruction

The artificial sky is supposed to have two main purposes: to diffuse the light and to prevent nonuniform reflections on the free-surface. Free-surface reconstruction attempts without any artificial sky gives no exploitable result, no matter the lighting conditions. When the **Config. 1** is fully set up, the reconstruction becomes possible using the natural surrounding light, but also using LED lighting heads in certain conditions (see **Section 3.3**). This brief study shows how the artificial sky works as a filter for surrounding parasite lights. In the wave and current facility of Boulogne-sur-Mer, less parasite lights were present as the room could go almost totally dark.

3.3. Influence of the direct/diffuse lighting

Now that the effects of the artificial sky are proven to be beneficial for the reconstruction, one can focus on the lighting set-up. Firstly, **Config. 1** is set up. With a will of lighting the free surface, from above, using the artificial sky, two LED lighting heads are set on tripods and oriented downwards, towards the artificial sky. Even with the largest aperture, the light is not diffused enough, and despite the translucent artificial sky, the lighting is not uniform on the free surface, creating shades differently seen from both cameras leading to low quality reconstructions. Moreover, no matter the location and orientation/angle of the lighting heads, when they are positioned only a few meters away from the artificial sky, the obtained reconstructions are not dense enough.

From these observations, we tried to create a more diffuse light by relocating both lighting heads further, at the end of the flume, about 35m from the artificial sky. **Fig. 9** shows a comparison of still free-surface reconstructions obtained with three different lighting set-ups, and schemes of the set-ups. In **Fig. 9.a**, both lighting heads are oriented horizontally with large aperture towards the artificial sky. The resulting reconstructions is completely unusable. Inspired by the lighting set-up used during the experimental campaign in Boulogne-sur-Mer, in **Fig. 9.b** the lighting heads are oriented in the opposite direction, to light a large reflective and diffusive surface, *i.e.*, a 5m x 3m metallic door. When surrounding lighting is strong enough, the free-surface is reconstructed, however, the point density is still not high and a huge gap appears

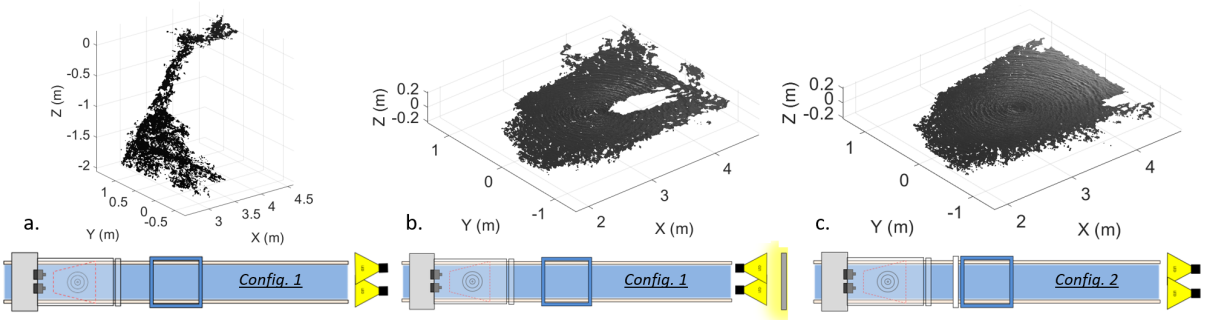

Figure 9. Still free-surface reconstruction comparison. a. Direct lighting. b. Indirect light (retro-lighting). c. WS illuminated by LED at the end of the flume.

in the middle of the reconstructed surface. As light intensity seems to be rather important for the reconstruction, we decided to bring the light source closer to the translucent artificial sky whilst keep a diffuse lighting. Consequently, **Config. 2** is set-up, and the opaque white screen is illuminated by both LED lighting heads from the flume end (see **Fig. 9.c**). The addition of the white screen creates a closer and more intense diffuse lighting, resulting in a free-surface reconstruction with a far better resolution and no gaps.

From this comparison one can sensibly assume that "direct" lighting is definitely to be avoided in contrast to diffuse lighting either using reflective lighting (like during the Boulogne-sur-mer campaign), or by means of the intermediary diffusive screen (**Config. 2**).

On **Fig. 9.b and 9.c**, it can be seen that reconstructions are less dense closer to the cameras. Indeed, short waves dissipate with distance from the source point, making the texture poorer. Moving the source point closer to the cameras allows to reconstruct an area that is closer to the cameras at the expense of the surface located further, confirming what have been observed in **Section 2.2**.

3.4. Translucent v.s. *Opaque artificial sky*

Now that the benefits of diffusing the light through an opaque white screen have been shown, one can focus on the comparison between regular waves reconstructions obtained when a translucent artificial sky with an opaque screen ahead (**Config. 2**) is set and when the artificial sky is made of opaque white screens (**Config. 3**).

Fig. 10 shows the reconstruction of regular waves with parameters H=0.048m, T=0.67s. The set-up for this reconstruction is exactly the same as the one pictured on **Fig. 9.c**, *i.e.*, two lighting head positioned at the end of the flume, illuminating the white screen in front of the translucent artificial sky. The left image on **Fig. 10** presents the raw reconstruction (untreated point cloud), while the right image is a reconstruction obtained by linear interpolation on a regular mesh ($\Delta x, \Delta y = 10mm$) and then the application of a z-coordinates median filter. The reconstruction is comparable to what was obtained at the end of the experimental campaign in Boulogne-sur-Mer (see **Section 2.3**) as the reconstructed surface is rather dense and large.

Fig. 11 shows a reconstruction made with **Config. 3**. It has the same wave parameters and same lighting heads configuration as used for **Fig. 10**. Nonetheless, less surface is reconstructed, and gaps appear behind the furthest crest while this phenomenon does not append in **Fig. 10**. It is due to an overexposure caused by direct lighting coming from a small gap between the white screen and the free-surface. In the case of (**Config. 2**), the translucent artificial sky filters this "direct light". Finally, the reconstruction seems laterally cropped compared to **Fig. 10**. The artificial sky being more opaque prevents surrounding light to brighten the surface, making the

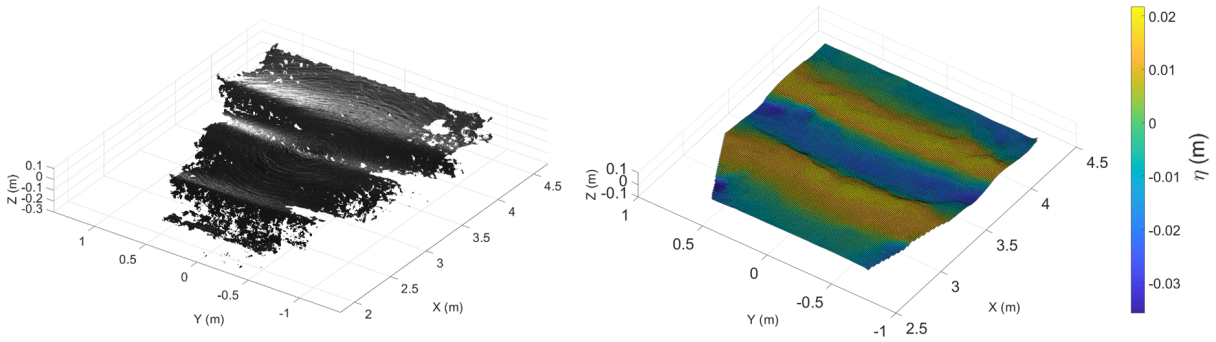

Figure 10. Regular Waves Reconstruction (H=0.048 , T=0.67s) with Config. 2. Left Image: Raw point cloud. Right Image: Linear Interpolation

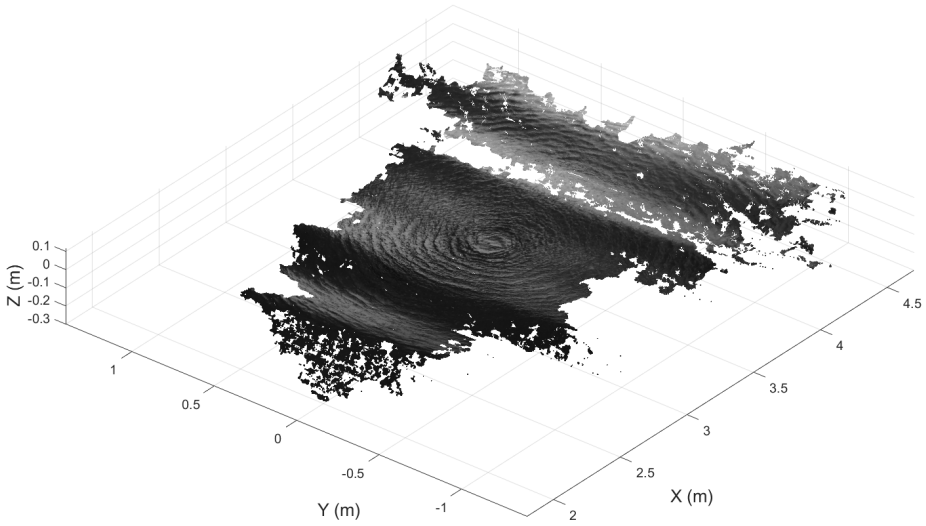

Figure 11. Regular Waves Reconstruction (H=0.048 , T=0.67s) with Config. 3.

front screen the only source of light and intensify shades from the side walls.

In contrast, although only one translucent screen was used to diffuse the light during the first experimental campaign in Boulogne-sur-Mer, the screen was wider than the flume, decreasing shades on the sides hence maximizing the reconstructed area.

To conclude this section, one can say that **Config. 2** seems to be the best configuration for waves reconstruction. The association of a translucent artificial sky and a diffusive white screen allows to have a diffuse and filtered lighting of the free-surface.

4. Generation of texture using Underwater Acoustics (UA)

With the purpose of generating texture at the free-surface without disturbing the generated waves (unlike compressed air projection), other texture generation ways have been investigated. UA is one of the considered options. As mentioned in [16],[17] and [18], ultrasonic acoustic emissions may generate short waves at the free-surface.

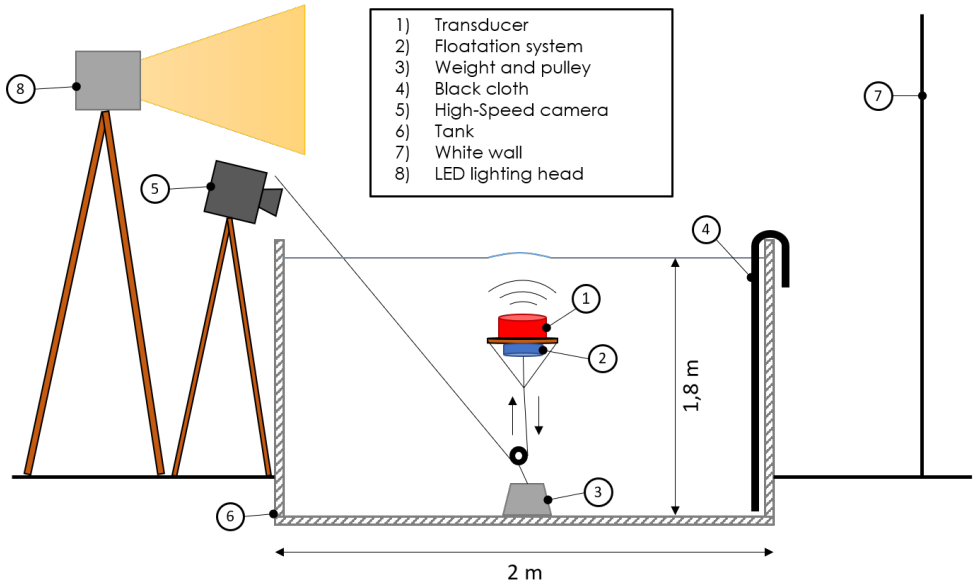

Figure 12. Experimental set-up for texture generation with ultrasonic transducers tests

4.1. Short waves generation using ultrasonic transducers

Table 2. Characteristics of tested SIMRAD® transducers

	ES 200-7C	ES 333-7C	ES 38-10
Nominal frequency	200 kHz	333 kHz	38 kHz
Frequency range	160-220 kHz	280-450 kHz	35-45 kHz
Beamwidth	7°	7°	10°
Dimensions (HxØ)	75x120 mm	75x120 mm	150x340 mm
Max. Input Power	1000 W	200 W	1500 W
Acoustic Power	227 dB	220 dB	227 dB
Max. Pulse Length	16 ms	16 ms	16 ms

To study this alternative, three underwater ultrasonic transducers have been tested (the characteristics of each transducers are described in **Tab.2**). The transducers can emit pulsed signals of adjustable duration. The period between each pulse is also adjustable but is of a minimum duration of about 100 times the pulse duration (amplifier's limit). Transducers can work in continuous wave mode (CW), emitting a signal with constant amplitude and frequency, and in frequency modulation mode (FM) where the frequency varies along a range over a pulse. **Fig. 12** shows a scheme of the experimental set-up used to observe free-surface short waves in a small tank (4m x 2m, 1.8m deep). Each transducer is plunged underwater with a system enabling depth change. In line with the previous stereo-video campaign, the lighting consist in illuminating a white wall, located on the opposite side of the cameras so the reflection contrasts the short waves generated by the transducers.

The first trials at a depth of 46cm show that both ES200-7C and ES333-7C emitting in CW mode at nominal frequency can generate a source point at the free-surface inducing gravity waves

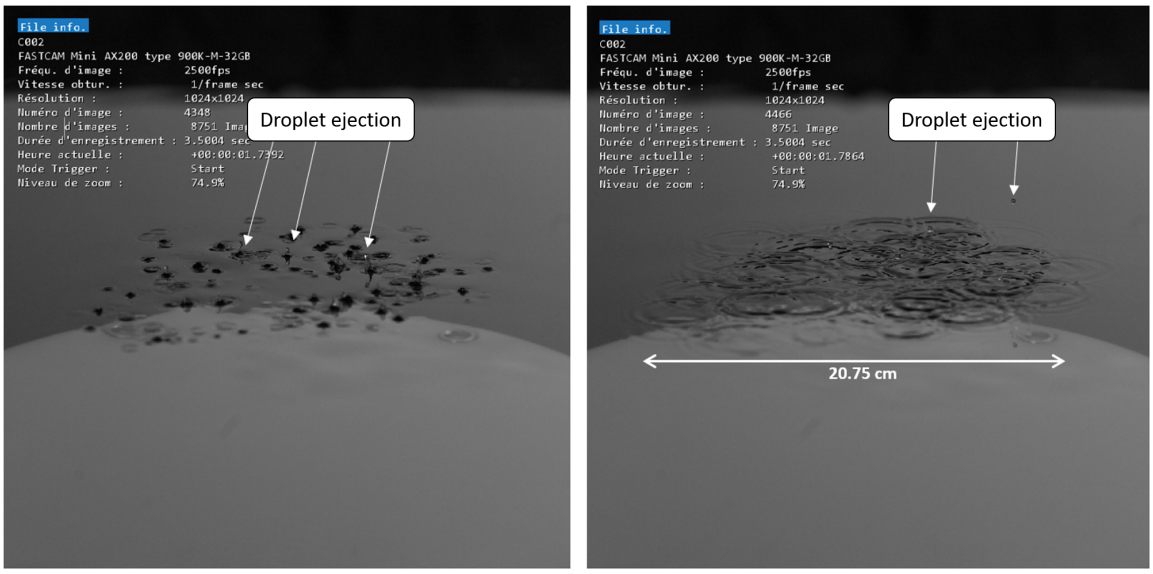

Figure 13. Shortwaves generated with ES38-10 (Depth: 21cm, Pulse Length: 8.192ms, Inter-Pulse: 2400ms, Mode: FM, Freq. Range: 35-45 kHz). Pictures taken 47 ms apart (from left to right)

with the period equals to the inter-pulse duration (time between two consecutive pulses). The amplitude of the generated gravity waves are higher with the ES200-7C than with the ES333-7C suggesting that more acoustic power creates more pressure under the surface. Limited by the amplifier capacity, one cannot set shorter inter-pulse duration, that would generate a finer texture. The generated gravity waves are not interesting since they propagate and disturb the free-surface too much.

When transducers are set at 21cm from the free-surface, one can observe an interesting shorter wave structure of about 5cm wide above the ES200-7C that is not present with the ES333-7C, confirming the idea that acoustic power has an impact on surface excitation. When ES38-10 is set-up 20cm deep, a similar but wider short wave structure (about 20 cm wide) is observable and shown in **Fig. 13**. Filming with high frame rate allows to observe first the appearance of many punctual free-surface elevation, energetic enough to expel droplets in the air (left image) and then in a second time, the appearance of short waves (right image). The observed short wave structure would make a decent texture if one could extend the affected surface. With few other tests it could be noticed that using FM mode, instead of CW mode, but also increasing the pulse duration make the short waves density increase. At 67cm deep, short waves are still present but not dense enough to be used for stereo-video. At 1.56m, no free-surface perturbation is observed.

These tests show that short waves generated by ultrasonic signal emissions seem highly dependant on the acoustic power of the used transducer and energy-intensive. The radius of the excited surface seems also to be proportional to the radius of the transducer. Unfortunately, the transducers used during these tests were only powerful enough to create interesting short waves at low depth (around 20cm), making their use only suitable for coastal test tanks. At reasonable depth for deeper wave tanks, from 1m, no short waves were discernible. It seems that more powerful with larger diameter transducers would be necessary. Knowing that the levels of emission used during the tests were already high, it raises the question about the feasibility of using short waves generated by ultrasonic signals as texture for stereo-video wave measurements.

4.2. "Stains" appearance using ultrasonic transducers

While testing short waves generation with the ES38-10, we observed the presence of "white stains" before the appearance of the punctual free-surface elevations, at depths of 20 cm, 67cm and even 1.56m (under different lighting conditions). On **Fig. 14**, one can observes the appearance and disappearance of the mentioned stains. Using a trigger on the signal emission to turn the camera recording on, one can notice that the stains appear right after a pulse emission and their appearance duration corresponds exactly to the emitted pulse duration. Continuously played, this record shows some stains moving, leading one to think that the stains could actually be bubbles.

Many articles mention the use of ultrasonic transducers to generate acoustic cavitation. Acoustic cavitation is described by Ashokkumar [19] as the growth and collapse of preexisting micro-bubbles under the excitation of an ultrasonic field. In fact, non degassed liquids contains microscopic dissolved gas nuclei that can grow and collapse or implode. According to Gugulothu *et al* [20], the use of piezoelectric transducer is the easiest way to yield acoustic cavitation. Frequencies associated to acoustic cavitation would range between 20 and 60 kHz which corresponds to the range swept through during tests with ES38-10. Furthermore, apparently higher frequencies can increase the bubble activity within the water column. High frequencies generated bubbles could act as nuclei for lower frequencies hence favoring acoustic cavitation. Liu & Hsieh [21] have experimentally demonstrated this theory showing that bubbles generated by acoustic cavitation occupy a larger space in the water column when stimulated at 83 kHz and 241 kHz simultaneously rather than separated. On our side, further observations show that the stain density increases with the pulse duration, along with the use of the FM mode instead of CW mode, which could correlate Liu & Hsieh [21] experience. Another explanation could be the fact that sweeping a range of frequencies would make bubble nuclei of difference sizes resonate hence increase the bubble activity in contrast to only one frequency making only bubbles of a certain size resonate.

So far, it is impossible to know whether the observed stains are actually bubbles generated by acoustic cavitation or not. Thus, it is not known if the observed phenomenon happens at, or close to, the free-surface, which, in this case, could make it attractive as a texture generation mean for stereo-video measurements.

5. Conclusion and prospects

Based on the results obtained during both stereo-video experimental campaigns, we have shown that it is possible to reconstruct the free-surface, indoor, using short waves as texture. We also showed that fine texture and correct lighting are indissociable to produce dense and accurate free-surface reconstructions. About the lighting, the campaign showed that direct lighting is to be avoided at all cost. The use of a translucent artificial sky over the reconstructed area to filter and diffuse surrounding lighting, combined with a large illuminated diffusive white screen, seems to be favorable to good reconstructions. However, with a very good texture, it is almost possible to reconstruct the free-surface everywhere, even with a lighting set-up with a low level of intensity.

Short-wave generation using ultrasonic transducers is a seducing approach as it is potentially less intrusive than compressed air blowing. However, it requires very high levels of emission to obtain exploitable texture at larger depths and on larger areas. In a near future, other tests will be performed on ultrasonic transducers in order to observe the location of the stains in the water column and see if they can be correlated to the punctual free-surface elevations responsible for the short waves generation.

Other ways of generating texture are to be investigated, as it is the most challenging aspect to improve in order to develop a robust and accurate stereo-video based free-surface reconstruction for wave tank experiments.

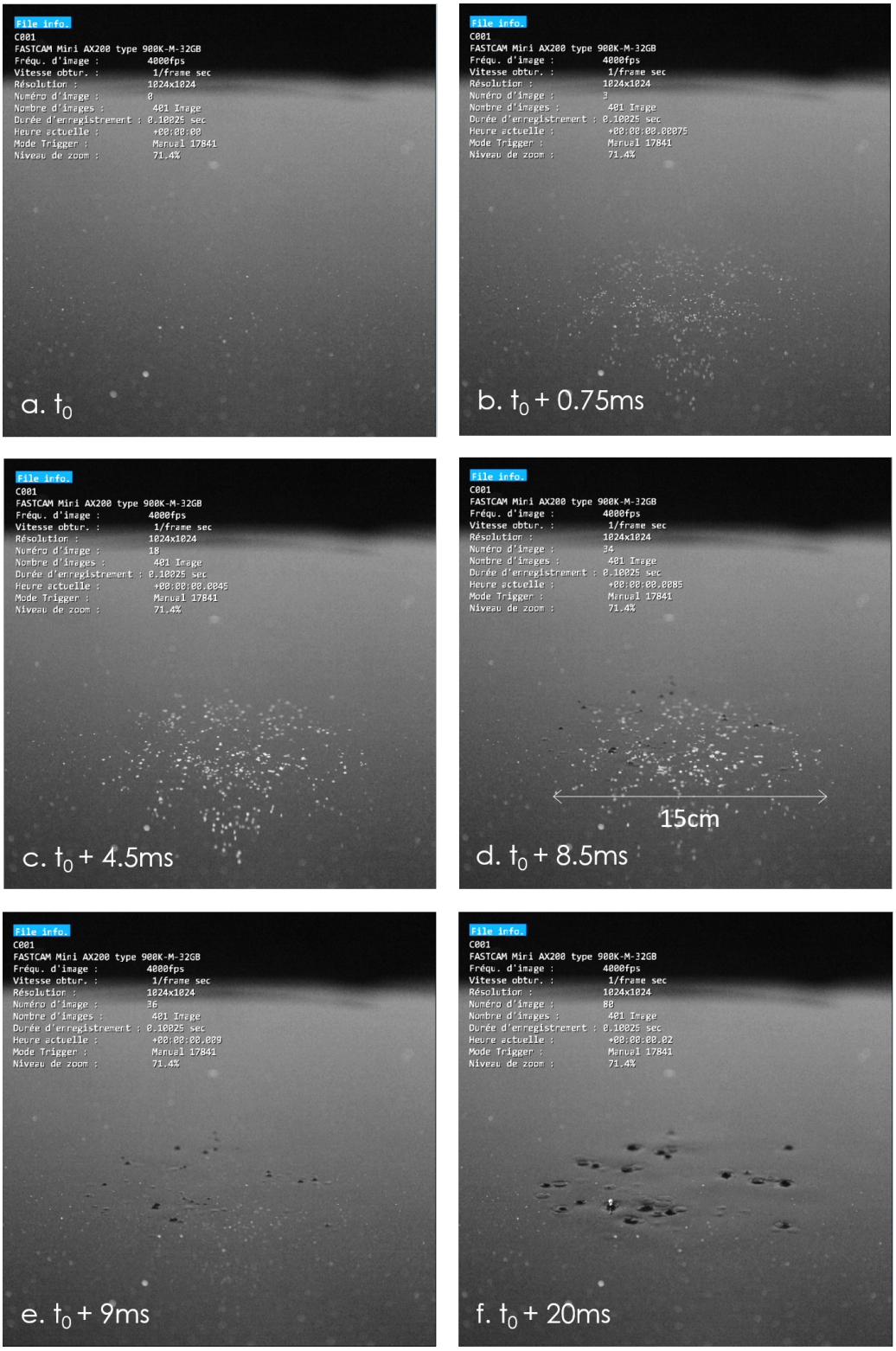

Figure 14. Free-surface evolution above ES38-10 from pulse emission (a. t_0) to short waves appearance (f. t_0+20ms) (Depth: 67 cm, Pulse Duration: 8.192 ms, Inter-pulse: 2400ms, Mode: FM, Freq. Range: 35-45 kHz)

Acknowledgments
This work has received funding from the Carnot Marine Engineering Research for Sustainable, Safe and Smart Seas Institute.

The authors would like to express their gratitude for help in anyway to: Tristan Adam, Thomas Baccheti, Sebastien Chalony, Benoit Gaurier, Jean-Valery Facq, Marie Ponchart, Naïg Le Bouffant and Laurent Berger. Special thanks are addressed to *ALL PURPOSE Roscoff* for the boat sails donation.

References

[1] Baldock T E and Swan C 1994 *Applied Ocean Research* **16** 101–112 ISSN 0141-1187 URL https://www.sciencedirect.com/science/article/pii/014111879490006X
[2] Craciunescu C C and Christou M 2019 Identifying Breaking Waves from Measured Time Traces (OnePetro) URL https://onepetro.org/ISOPEIOPEC/proceedings-abstract/ISOPE19/All-ISOPE19/21000
[3] Swan C and Sheikh R 2015 *Philosophical Transactions of the Royal Society A: Mathematical, Physical and Engineering Sciences* **373** 20140114 publisher: Royal Society URL https://royalsocietypublishing.org/doi/10.1098/rsta.2014.0114
[4] Hulin F, Tassin A, Filipot J F and Jacques N 2022 Experimental investigation of the hydrodynamic loads induced by breaking wave impacts on a SPAR-type floating offshore wind turbine URL https://jh2022.sciencesconf.org/420514
[5] Lubin P, Kimmoun O, Véron F and Glockner S 2019 *European Journal of Mechanics - B/Fluids* **73** 144–156 ISSN 0997-7546 URL https://www.sciencedirect.com/science/article/pii/S0997754617302881
[6] Aubourg Q, Campagne A, Peureux C, Ardhuin F, Sommeria J, Viboud S and Mordant N 2017 *Physical Review Fluids* **2** 114802 publisher: American Physical Society URL https://link.aps.org/doi/10.1103/PhysRevFluids.2.114802
[7] Gomit G, Chatellier L, Calluaud D and David L 2013 *Experiments in Fluids* **54** 1540 ISSN 1432-1114 URL https://doi.org/10.1007/s00348-013-1540-4
[8] Savelyev I and Fuchs J 2018 *Frontiers in Mechanical Engineering* **4** ISSN 2297-3079 URL https://www.frontiersin.org/articles/10.3389/fmech.2018.00001
[9] Bergamasco F, Torsello A, Sclavo M, Barbariol F and Benetazzo A 2017 *Computers & Geosciences* **107** 28–36 ISSN 0098-3004 URL https://www.sciencedirect.com/science/article/pii/S0098300417304302
[10] Benetazzo A 2006 *Coastal Engineering* **53** 1013–1032 ISSN 0378-3839 URL https://www.sciencedirect.com/science/article/pii/S0378383906000962
[11] Benetazzo A, Fedele F, Gallego G, Shih P C and Yezzi A 2012 *Coastal Engineering* **64** 127–138 ISSN 0378-3839 URL https://www.sciencedirect.com/science/article/pii/S0378383912000166
[12] MATLAB 2023 Estimate geometric parameters of a stereo camera - MATLAB - MathWorks France URL https://fr.mathworks.com/help/vision/ref/stereocameracalibrator-app.html
[13] Bouguet J Y 2008 Camera Calibration Toolbox for Matlab URL http://robots.stanford.edu/cs223b04/JeanYvesCalib/
[14] Zhang Z 2000 *IEEE Transactions on Pattern Analysis and Machine Intelligence* **22** 1330–1334 ISSN 1939-3539 conference Name: IEEE Transactions on Pattern Analysis and Machine Intelligence
[15] Heikkila J and Silven O 1997 A four-step camera calibration procedure with implicit image correction *Proceedings of IEEE Computer Society Conference on Computer Vision and Pattern Recognition* pp 1106–1112 iSSN: 1063-6919
[16] Krutyansky L, Preobrazhensky V, Makalkin D, Brysev A and Pernod P 2020 *Ultrasonics* **100** 105972 ISSN 0041-624X URL https://www.sciencedirect.com/science/article/pii/S0041624X19300344
[17] Boubekri R, Gross M, In M, Diat O, Nobili M, Möhwald H and Stocco A 2016 *Langmuir: the ACS journal of surfaces and colloids* **32** 10177–10183 ISSN 1520-5827
[18] Prokhorov V E and Chashechkin Y D 2009 *Izvestiya, Atmospheric and Oceanic Physics* **45** 495–502 ISSN 1555-628X URL https://doi.org/10.1134/S0001433809040094
[19] Ashokkumar M 2011 *Ultrasonics Sonochemistry* **18** 864–872 ISSN 1350-4177 URL https://www.sciencedirect.com/science/article/pii/S1350417710002312
[20] Gugulothu S K, Kumar P R V and Deekshith P 2012 *Procedia Engineering* **38** 154–164 ISSN 1877-7058 URL https://www.sciencedirect.com/science/article/pii/S1877705812019352
[21] Liu H L and Hsieh C M 2009 *Ultrasonics Sonochemistry* **16** 431–438 ISSN 1350-4177 URL https://www.sciencedirect.com/science/article/pii/S1350417708001508